The Astrophysical Journal, 884:27 (6pp), 2019 October 10 https://doi.org/10.3847/1538-4357/ab3e0c


# Neutrino-driven Instability of Ion Acoustic Waves in an Ultrarelativistic Degenerate Plasma

Yashika Ghai[1], N. S. Saini[1], and B. Eliasson[2]
[1] Department of Physics, Guru Nanak Dev University, Amritsar-143005, India; nssaini@yahoo.com
[2] SUPA, Department of Physics, University of Strathclyde, Glasgow G4 ONG, UK
*Received 2019 January 19; revised 2019 August 19; accepted 2019 August 19; published 2019 October 8*

## Abstract

The coupling between ion acoustic waves (IAWs) and a neutrino beam undergoing flavor oscillations in a dense, relativistically degenerate plasma is analyzed. The neutrino-driven streaming instability of the IAWs is investigated with relevance to plasma conditions at the last stage of stellar evolution in a massive supernova progenitor. The influence of neutrino beam parameters such as the energy of the incident neutrino beam and eigenfrequency of the neutrino flavor oscillations on the instability growth rate is obtained numerically. It is observed that the neutrino flavor oscillations significantly affect the neutrino-driven instability of the IAWs. Our results also indicate that the time period for the onset of the streaming neutrino-driven instability is shorter than the typical time period of a core-collapse supernova explosion. The findings of this investigation may shed new light on the understanding of the underlying physical mechanism responsible for the core-collapse supernova.

*Unified Astronomy Thesaurus concepts:* Supernova neutrinos (1666); Neutrino oscillations (1104); Core-collapse supernovae (304); Degenerate matter (367); Relativistic fluid dynamics (1389); Plasma physics (2089)

## 1. Introduction

The mechanism of a core-collapse supernova due to the gravitational death of a massive star is considered to be one of the most complex and physically rich astrophysical phenomena (Jankaa et al. 2007). The investigation of a supernova comprises the study of plasma dynamics in a strong gravitational field while considering the transport of intense neutrino beams from the core to the outer layers of the supernova progenitor. At the advanced stages of stellar evolution, the electron–positron pair annihilation is the main process responsible for the production of neutrinos. However, during the collapsing stage, electron capture by the Fe-peak elements becomes the dominant neutrino emission process. If the mean-free path of these neutrinos is much shorter than the size of the dense core of the star, the neutrinos interact with the core a number of times before diffusing out of the core (Mezzacappa & Messer 1999). The interaction of neutrinos with the core plasma may lead to different kinds of hydrodynamic instabilities in the supernova core during the first few seconds of the explosion. These instabilities are of potential importance as they may trigger the explosion, or create the seed for the ejecta asymmetries observed later on.

Due to their critical role in the energy and momentum transfer that causes the Supernova II (SN II), several authors have over the past few decades investigated the nonlinear interaction of intense neutrino beams with plasmas (Chiueh 1993; Bingham et al. 1994, 1996; Serbeto 1999; Shukla et al. 1999; Silva et al. 1999, 2000; Serbeto et al. 2002). Quantum mechanically, it is proposed that a neutrino spends some of its time as a combination of two virtual particles, one of which is an electron and the other a $W^+$-boson. The motion of neutrinos through the plasma tends to influence these virtual charged particles, which leads to a form of inhomogeneous Debye shielding of the particles, thus giving rise to a net electric charge and the induced electromagnetic properties of the neutrinos in plasma. The small neutrino charge in plasma is given by $G_{j\nu} = \sqrt{2}\,G_{\rm F}(\delta_{je}\delta_{\nu\nu_e} + (I_j - 2Q_j \sin^2\theta_w))$, where $j$ denotes the electron ($e$) and proton ($p$) species of plasma, $G_F$ is the Fermi's coupling constant of weak interaction, $\theta_w$ is the Weinberg mixing angle ($\sin^2\theta_w \approx 0.23$), $I_j$ is the weak isotopic spin of the particle of species $j$ (equals $-1/2$ for electrons and $+1/2$ for protons), and $Q_j = q_j/e$ is the particle normalized electric charge. A weakly charged neutrino beam propagating through a dense plasma interacts with the plasma electrons via electro–weak interaction and may give rise to a neutrino-driven instability.

Bingham et al. (1994) studied the collective interactions between dense plasmas and neutrinos emitted in the core of a supernova. They showed that an intense neutrino beam couples nonlinearly with collective plasma oscillations, which leads to the transfer of neutrino energy to Langmuir waves that further heat the plasma electrons through collisional damping. Another analysis by Chiueh (1993) showed that the interaction of neutrinos with ion sound waves gives rise to a neutrino-driven instability, and the instability growth rate scales as $\approx G_{\rm F}$. The instability growth rate dominates over the viscous damping of the sound waves and leads to a net growth of the instability. The detailed physics of collective interactions between neutrinos and plasmas has been highlighted (Shukla et al. 1999), and it has been shown that an intense neutrino beam may lead to two-stream instabilities, inhomogeneities, and magnetic fields in plasmas. Serbeto et al. (2002) used a hydrodynamic description to analyze the ion sound wave excitation by intense neutrino beams. They obtained a neutrino-modified dispersion relation for the ion sound waves and proposed that the generated ion waves may be responsible for the energy–momentum transfer from neutrinos to the plasma environment of SN II that can enhance the stalled supernova shocks.

Depending upon the properties of the medium through which neutrinos propagate, there occurs a two-way periodic transformation of one type of neutrino into another (Mikheev & Smirnov 1986, 1987; Smirnov 2005). This phenomenon, referred to as a neutrino flavor oscillation, was found to be responsible for the solar-neutrino deficit problem (Bethe 1986). When the neutrinos interact with plasma, it causes a resonant coupling between different flavor states. Recently, researchers

have investigated the interaction of a neutrino beam with plasma while considering the effect of neutrino flavor oscillations (Mendonça & Haas 2013; Mendonça et al. 2014; Haas et al. 2017a, 2017b). Mendonça & Haas (2013) introduced a new model for the joint neutrino flavor and plasma oscillations by formulating a neutrino flavor polarization vector in a plasma. Mendonça et al. (2014) found that the electron plasma waves excited by the intense neutrino beams are linked with the flavor oscillations of neutrinos, and that the dispersion relation and growth rates of neutrino-driven instabilities are directly influenced by the flavor oscillations.

The plasmas present in the core of a star at the last stages of stellar evolution as well as in white dwarf interiors, neutron stars, etc., are dense with electron number densities greater than $10^{30}$ cm$^{-3}$. At such high number densities, the Fermi energy of electrons is greater than the thermal energy, i.e., $E_{\rm Fe} > K_B T_e$ and the electrons are degenerate. Hence, it becomes important to incorporate the quantum effects such as electron degeneracy pressure while analyzing the instability phenomenon in a dense astrophysical plasma. On the other hand, relativistic effects depend upon the relative magnitudes of the Fermi energy of the electron fluid and the rest mass energy of electrons. In other words, if $E_{\rm Fe} > m_e c^2$, the charged species are considered to be relativistic. In a classic paper, Chandrasekhar (1935) specified the form of the degeneracy pressure in a dense plasma ranging from the nonrelativistic to the ultrarelativistic limits. Haas (2016) presented a detailed theoretical description of the model equations suitable for an ultrarelativistic degenerate plasma by comparing the expressions for the dispersion relation of ion acoustic waves using both fluid and kinetic approaches. In the prolific plasma literature, various authors have analyzed the ion acoustic waves in dense astrophysical plasmas while taking into account the relativistic and degenerate character of the electrons (Eliasson & Shukla 2012; Masud & Mamun 2013; Haas 2016; Rahman et al. 2017; Iqbal et al. 2018; Sharma 2018). Haas & Eliasson (2015) presented a study of a two-stream instability mode in a magnetized plasma while considering a quantum hydrodynamic model. The authors reported a new transverse model of streaming instability due to streaming electron beams having properties of a nonrelativistic dense Fermi gas and immobile ions in the presence of an external magnetic field. An investigation of ion acoustic waves was reported by Khan et al. (2016) in an extremely dense, magnetized, astrophysical plasma containing nonrelativistic ions and relativistic degenerate electrons. They analyzed the dispersive effects due to plasma density and magnetic field strength on the triggering of ion acoustic waves (IAWs) in very high density plasmas under extreme conditions. Prajapati (2017) reported the analysis of neutrino-beam-driven instability in a homogeneous, self-gravitating, quantum plasma in the presence of a neutrino beam, but where the influence of neutrino flavor oscillations was not taken into consideration.

Due to the slow nature of both the neutrino flavor oscillations and the IAWs, it is interesting to investigate the resonance between IAWs and neutrino flavor oscillations. Haas et al. (2017a) studied the coupling between IAWs and neutrino oscillations in a nonrelativistic electron–ion plasma in context with the observations of supernova 1987A (Hirata et al. 1987). They concluded that the neutrino flavor oscillations excite a new fast unstable mode by transfer of energy to the plasma in extreme astrophysical scenarios. Further, it has been reported that the coupling between neutrino flavor oscillations and the IAWs in a completely ionized plasma is not influenced by the collisional effects (Haas et al. 2017b). It is a well-established fact that a massive star after exhausting all of its nuclear fuel contracts under its own gravitational pull until it reaches a stage when there is an abundance of iron nuclei as the major trace element and the electrons are relativistic as well as degenerate. Many theoretical and simulation studies (Connor 2015; Fröhlich et al. 2018; Ott et al. 2018) have investigated the neutrino-beam-driven instability mechanism responsible for a core-collapse supernova in a supernova progenitor.

The motivation of the present investigation is to explore the dynamics of supernova explosion via the neutrino–plasma interaction process in the dense, degenerate core of a supernova progenitor star, including the impact of neutrino flavor oscillations on the neutrino-driven instability of the IAWs in a dense astrophysical plasma such as that at the last stage of stellar evolution comprising ultrarelativistic degenerate electrons and nondegenerate ions. It is expected that if a supernova explosion occurs at a distance of ∼100 pc, the neutrinos emitted in the process may be detected by the neutrino detector KamLAND (Yoshida et al. 2016). In the present study, we have investigated an instability regime of neutrino-driven streaming instability with predicted parameters for a supernova explosion in a progenitor star. We have highlighted the effects of eigenfrequency of the neutrino flavor oscillations on the growth rate of the instability and the influence of different physical parameters that are characteristics of the streaming neutrino beam and the plasma environment. Our investigation gives a broader understanding of the instabilities in dense astrophysical environments such as degenerate cores of massive stars, which may seed or influence the dynamics of the core collapse in a supernova progenitor.

The paper is structured as follows: Section 2 presents the fluid model equations. A dispersion relation for ion acoustic waves in a relativistic degenerate plasma in the presence of a neutrino beam with flavor oscillations is derived in Section 3, which is analyzed in Section 4 with respect to the neutrino beam instability. Finally, concluding remarks are given in Section 5.

## 2. Fluid Model Equations of Plasma and Neutrino Beam

Using a neutrino-modified fluid approach, we investigate the instability of IAWs in an unmagnetized, dense plasma containing cold heavy ions and ultrarelativistic degenerate electrons interacting with a neutrino beam undergoing two-flavor oscillations. The continuity and momentum equations for the ions are written in the relativistic form as

$$\frac{\partial(\gamma_i n_i)}{\partial t} + \nabla \cdot (\gamma_i n_i \boldsymbol{u}_i) = 0, \tag{1}$$

$$m_i n_i \left(\frac{\partial}{\partial t} + \boldsymbol{u}_i \cdot \nabla\right)(\gamma_i \boldsymbol{u}_i) = -q_i n_i \nabla \phi, \tag{2}$$

where $n_i$ and $\boldsymbol{u}_i$ are, respectively, the proper number density and velocity of the ion fluid, $\gamma_i = (1 - u_i^2/c^2)^{-1/2}$ is the relativistic factor for ions, $m_i$ depicts the mass of the ion species, $\phi$ is the electrostatic potential, and $q_i = Z_i e$ is the ion charge, where $Z_i$ is the ion charge number. The electron dynamics is modeled using a relativistic form of the electron

continuity and momentum equations,

$$\frac{\partial(\gamma_e n_e)}{\partial t} + \nabla \cdot (\gamma_e n_e \boldsymbol{u}_e) = 0, \tag{3}$$

$$m_e H\left(\frac{\partial}{\partial t} + \boldsymbol{u}_e \cdot \nabla\right)(\gamma_e \boldsymbol{u}_e) = -\frac{\gamma_e}{n_e}\left(\nabla + \frac{\boldsymbol{u}_e}{c^2}\frac{\partial}{\partial t}\right)P_{\rm Fe} + e\nabla\phi + \sqrt{2}\,G_{\rm F}(\boldsymbol{E}_\nu + \boldsymbol{u}_e \times \boldsymbol{B}_\nu), \tag{4}$$

where $\gamma_e = (1 - {u_e}^2/c^2)^{-1/2}$ is the relativistic factor for electrons and $H$ is the non-dimensional enthalpy density defined as $H = \sqrt{1+\xi^2}$, where $\xi = \hbar\,(3\pi^2 n_{e0})^{1/3}/m_e c$. For the ultrarelativistic degenerate electrons $\xi^2 \gg 1$, so that $H \approx \xi$. For the slowly evolving IAWs, the electrons are considered to be inertialess, so the terms on the left-hand side of Equation (4) will be omitted below. The electron Fermi pressure is given by Chandrasekhar's ultrarelativistic equation of state (Chandrasekhar 1935) as $P_{\rm Fe} = \left(\frac{3}{\pi}\right)^{1/3}\frac{hc}{8}{n_e}^{4/3}$, where $h$ is Planck's constant and $c$ is the speed of light. Here, $n_e$ and $\boldsymbol{u}_e$ are the proper number density and velocity of the electron fluid. In Equation (4), $G_F$ is the Fermi's coupling constant of weak interactions, and the neutrino's effective weak electric and magnetic fields are given by

$$\boldsymbol{E}_\nu = -\nabla N_e - \frac{1}{c^2}\frac{\partial}{\partial t}(N_e \boldsymbol{v}_e) \quad \text{and} \quad \boldsymbol{B}_\nu = \frac{1}{c^2}\nabla \times (N_e \boldsymbol{v}_e), \tag{5}$$

respectively, where $N_e$ is the number density, $\boldsymbol{v}_e$ is the fluid velocity of electron neutrinos, and $c$ is the speed of light. It should be noted that the Fermi's weak force couples the electron neutrinos with the electrons (leptons) only and not with the ions (hadrons). The system of equations is closed by Poisson's equation

$$\nabla^2\phi = \frac{e}{\epsilon_0}(\gamma_e n_e - Z_i\gamma_i n_i), \tag{6}$$

where $\epsilon_0$ is the electric permittivity of vacuum. We here consider large-scale ion acoustic waves, where the electrons stream to neutralize the ions, so that Poisson's Equation (6) can be replaced by the quasi-neutrality condition $\gamma_i Z_i n_i = \gamma_e n_e$. Also, for IAWs the electron and ion fluid velocities are nonrelativistic, and hence the relativistic gamma factors ($\gamma_i$ and $\gamma_e$) are reduced to $\approx$1.

In order to investigate the coupling between plasma and neutrino oscillations, we consider two-flavor neutrino oscillations and, hence, represent the continuity equations for the electron and muon-neutrino in terms of the quantum coherence factor

$$\frac{\partial N_e}{\partial t} + \nabla \cdot (N_e \boldsymbol{v}_e) = \frac{1}{2}N\Omega_0 P_2, \tag{7}$$

$$\frac{\partial N_\mu}{\partial t} + \nabla \cdot (N_\mu \boldsymbol{v}_\mu) = -\frac{1}{2}N\Omega_0 P_2, \tag{8}$$

where $N = N_e + N_\mu$ is the total neutrino fluid density, $N_\mu$ and $\boldsymbol{v}_\mu$ are the muon-neutrino fluid density and velocity, respectively, and $P_2$ is the quantum coherence factor in the flavor polarization vector $\boldsymbol{P} = (P_1, P_2, P_3)$. Also, $\Omega_0 = \omega_0 \sin 2\theta_0$, where $\omega_0 = \Delta m^2 c^4/2\mathcal{E}_0$, $\Delta m^2$ is the squared neutrino mass difference, $\mathcal{E}_0$ is the neutrino spinor's energy in the fundamental state, and $\theta_0$ is the neutrino oscillation mixing angle. The terms on the right-hand side of Equations (7)–(8) with the opposite sign depict the contribution from neutrino oscillations to the rate of change in electron and muon-neutrino density flows. The global density of neutrinos is conserved as

$$\frac{d}{dt}\int (N_e + N_\mu)d\boldsymbol{r} = -\int \nabla.(N_e \boldsymbol{v}_e + N_\mu \boldsymbol{v}_\mu)d\boldsymbol{r} = 0, \tag{9}$$

where the volume integrals are over all space. The neutrino dynamics is modeled by the relativistic momentum equations

$$\left(\frac{\partial}{\partial t} + \boldsymbol{v}_e.\nabla\right)\boldsymbol{p}_e = \sqrt{2}\,G_{\rm F} \times \left(-\nabla n_e - \frac{1}{c^2}\frac{\partial}{\partial t}(n_e \boldsymbol{u}_e) + \frac{\boldsymbol{v}_e}{c^2} \times (\nabla \times n_e \boldsymbol{u}_e)\right), \tag{10}$$

$$\frac{\partial \boldsymbol{p}_\mu}{\partial t} + (\boldsymbol{v}_\mu \cdot \nabla)\boldsymbol{p}_\mu = 0, \tag{11}$$

where $\boldsymbol{p}_{e,\mu} = \mathcal{E}_{e,\mu}\boldsymbol{v}_{e,\mu}/c^2$ are the relativistic momenta of the electron and muon neutrinos and $\mathcal{E}_{e,\mu} = m_\nu c^2(1 - {v_{e,\mu}}^2/c^2)^{-1/2}$ are the energies of the electron and muon-neutrino beams. The time evolution of the flavor polarization vector in a material medium is given by

$$\frac{\partial P_1}{\partial t} = -\Omega(n_e)P_2, \qquad \frac{\partial P_2}{\partial t} = \Omega(n_e)P_1 - \Omega_0 P_3, \quad \text{and} \quad \frac{\partial P_3}{\partial t} = \Omega_0 P_2. \tag{12}$$

where $\Omega(n_e) = \omega_0(\cos 2\theta_0 - \sqrt{2}\,G_{\rm F} n_e/\hbar\omega_0)$.

## 3. Small Amplitude Wave Dispersion Relation

We linearize Equations (1)–(12) by considering plane wave perturbations of the form $f = f_0 + \delta f \exp(\iota(\boldsymbol{k}\cdot\boldsymbol{r} - \omega\boldsymbol{t}))$ with $|\delta f| \ll f_0$, where $f$ represents a physical quantity. The equilibrium values of the physical quantities for a homogeneous static equilibrium are (Haas et al. 2017a)

$$n_{e0} = Z_i n_{i0}, \quad \boldsymbol{u}_{e0,i0} = 0, \quad \phi = 0, \quad N_e = N_{e0}, \quad N_\mu = N_{\mu 0}, \quad \boldsymbol{v}_e = \boldsymbol{v}_\mu = \boldsymbol{v}_0. \tag{13}$$

Also, for the flavor polarization vector, we consider

$$P_{01} = \frac{\Omega_0}{\Omega_\nu},\ P_{02} = 0,\ P_{03} = \frac{\Omega(n_{e0})}{\Omega_\nu} = \frac{N_{e0} - N_{\mu 0}}{N_0}. \tag{14}$$

Here, we have $\Omega_\nu^2 = \Omega^2(n_{e0}) + \Omega_0^2$, where $\Omega_\nu$ represents the eigenfrequency of two-flavor neutrino oscillations and $N_0 = N_{e0} + N_{\mu 0}$ is the total equilibrium number density of the neutrino beam. The equilibrium values for the flavor polarization are obtained from the properties of neutrino oscillations in a fixed homogeneous medium, where it is considered that $\nabla = 0$. Also, by using that $Z_i\delta n_i = \delta n_e$, we substitute the expression for the electrostatic potential $\phi$ from the ion momentum equation in the electron momentum equation. The linearized electron momentum Equation (4) after taking its scalar product with $\boldsymbol{k}$ becomes

$$(\omega^2 - V_s^2 k^2)\delta n_e + \frac{\sqrt{2}\,G_{\rm F} Z_i n_{e0}}{m_i c^2} \times ((\omega\boldsymbol{k}\cdot\boldsymbol{v}_0 - c^2k^2)\delta N_e + \omega N_{e0}\boldsymbol{k}\cdot\delta\boldsymbol{v}_e) = 0. \tag{15}$$

where $V_s = \sqrt{Z_i\hbar c(3\pi^2 n_{e0})^{1/3}/3m_i}$ is the ion acoustic speed in the ultrarelativistic degenerate plasma. Linearizing the electron

neutrino momentum Equation (10), we obtain

$$c^2(\omega - \boldsymbol{k}\cdot\boldsymbol{v}_0)\delta\boldsymbol{p}_e = \mathcal{E}_0(\omega - \boldsymbol{k}.\boldsymbol{v}_0)\delta\boldsymbol{v}_e + \mathcal{E}_0(\omega - \boldsymbol{k}.\boldsymbol{v}_0)\left(1 - \frac{v_0^2}{c^2}\right)^{-1}\left(\frac{\boldsymbol{v}_0\cdot\delta\boldsymbol{u}_e}{c^2}\right) = \frac{\sqrt{2}}{c^2}G_{\rm F}(c^2\boldsymbol{k}\delta n_e - \omega n_{e0}\delta\boldsymbol{u}_e - n_{e0}(\boldsymbol{v}_0\times(\boldsymbol{k}\times\delta\boldsymbol{u}_e))). \quad (16)$$

where $\mathcal{E}_0 \equiv \mathcal{E}_{e0}$ is the energy of the incident electron neutrino beam. From Equation (16), we obtain the perturbed electron neutrino beam velocity

$$\delta\boldsymbol{v}_e = \frac{\sqrt{2}\,G_{\rm F}}{\mathcal{E}_0(\omega - \boldsymbol{k}\cdot\boldsymbol{v}_0)}(c^2\boldsymbol{k}\delta n_e - \omega n_{e0}\delta\boldsymbol{u}_e - \left((\boldsymbol{k}\cdot\boldsymbol{v}_0)\delta n_e - \frac{\omega n_{e0}}{c^2}\boldsymbol{v}_0\cdot\delta\boldsymbol{u}_e\right)\boldsymbol{v}_0 - n_{e0}((\boldsymbol{v}_0\cdot\delta\boldsymbol{u}_e)\boldsymbol{k} - (\boldsymbol{k}\cdot\boldsymbol{v}_0)\delta\boldsymbol{u}_e)). \quad (17)$$

The linearization of electron continuity Equation (3) yields the perturbed electron velocity

$$\delta\boldsymbol{u}_e = \frac{\omega\boldsymbol{k}\delta n_e}{n_{e0}k^2}. \quad (18)$$

Using Equation (18) in Equation (17), we obtain

$$\delta\boldsymbol{v}_e = \frac{\sqrt{2}\,G_{\rm F}}{\mathcal{E}_0(\omega - \boldsymbol{k}\cdot\boldsymbol{v}_0)}\left(1 - \frac{\omega^2}{c^2k^2}\right)(c^2\boldsymbol{k} - (\boldsymbol{k}\cdot\boldsymbol{v}_0)\boldsymbol{v}_0)\delta n_e. \quad (19)$$

Using Equation (19) with Equation (15), we find

$$(\omega^2 - V_s^2k^2)\delta n_e + \frac{\sqrt{2}\,G_{\rm F}n_{e0}Z_i}{m_ic^2}(\omega\boldsymbol{k}\cdot\boldsymbol{v}_0 - c^2k^2)\delta N_e + \frac{2G_{\rm F}{}^2N_{e0}n_{e0}Z_i\omega}{m_ic^2\mathcal{E}_0(\omega - \boldsymbol{k}\cdot\boldsymbol{v}_0)}\left(1 - \frac{\omega^2}{c^2k^2}\right)(c^2k^2 - (\boldsymbol{k}\cdot\boldsymbol{v}_0)^2)\delta n_e = 0. \quad (20)$$

On the other hand, from the electron neutrino continuity Equation (7), we have

$$(\omega - \boldsymbol{k}\cdot\boldsymbol{v}_0)\delta N_e - N_{e0}k\cdot\delta\boldsymbol{v}_e = \frac{\iota N_0\Omega_0\delta P_2}{2}. \quad (21)$$

The effect of neutrino oscillations is given by the $\delta P_2$ term in Equation (21); hence, we obtain the expression for the perturbation of quantum coherence vector from Equation (12) as

$$\delta P_2 = -\iota\frac{\sqrt{2}\,\Omega_0\omega G_{\rm F}\delta n_e}{(\omega^2 - \Omega_\nu{}^2)\hbar\Omega_\nu}. \quad (22)$$

By substituting Equations (19), (20), and (22) in Equation (21), we finally obtain the dispersion relation for IAWs in an ultrarelativistic degenerate plasma in the presence of a neutrino beam with flavor oscillations as

$$\omega^2 = V_s^2k^2 + A\frac{\Omega_0{}^2\omega(c^2k^2 - \omega(\boldsymbol{k}\cdot\boldsymbol{v}_0))}{\hbar\Omega_\nu(\omega - \boldsymbol{k}\cdot\boldsymbol{v}_0)(\omega^2 - \Omega_\nu{}^2)} + B\left(1 - \frac{v_0{}^2\cos^2\theta}{c^2}\right)\frac{2c^2k^2(c^2k^2 - \omega^2)}{\mathcal{E}_0(\omega - \boldsymbol{k}\cdot\boldsymbol{v}_0)^2}, \quad (23)$$

where

$$A = \frac{Z_iG_{\rm F}{}^2N_{e0}n_{e0}}{m_ic^2} \quad \text{and} \quad B = \frac{Z_iG_{\rm F}{}^2N_0n_{e0}}{m_ic^2}. \quad (24)$$

## 4. Analysis of Neutrino Beam Instability

For the neutrino beam mode, it is clear from the dispersion relation (23) that the growth rate is the maximum for the following resonance condition:

$$\omega \approx V_sk = \Omega_\nu = \boldsymbol{k}\cdot\boldsymbol{v}_0. \quad (25)$$

Let us consider the case when $\omega = \Omega_\nu + \delta\omega$, where $\delta\omega \ll \Omega_\nu$. By substituting these conditions in the general dispersion relation (23), we obtain the following equation:

$$2\Omega_\nu\,\delta\omega^3 - V_{\rm osc}\,\delta\omega - (V_{\rm beam} + \Omega_\nu V_{\rm osc}) = 0, \quad (26)$$

where $V_{\rm beam} = \frac{2Bc^4k^4}{\mathcal{E}_0}\left(1 - \frac{v_0{}^2\cos^2\theta}{c^2}\right)$ and $V_{\rm osc} = \frac{A\Omega_0{}^2c^2k^2}{2\hbar\Omega_\nu{}^2}$ are terms contributed by the neutrino beam and the neutrino flavor oscillations, respectively. We have numerically solved Equation (26) to find the growth rate $\delta\omega_{\rm img}$ of the neutrino-beam-driven instability. It is clear that the conditions (25) are met only for perturbation wavenumber of the order $\sim\Omega_\nu/V_s$, giving large-wavenumber or short-wavelength perturbations.

For the numerical analysis, we have used the parameters at the core-collapse stages of a massive star such as Betelgeuse, as given in a study by Yoshida et al. (2016), of time evolution of the neutrino spectra emitted from supernova progenitors. The values of various plasma parameters for iron plasma at the core-collapse stage of a progenitor star are considered as $\mathcal{E}_0 = 1.94$ MeV, $|\boldsymbol{v}_0| = 0.998c$, $N_0 = 1.013\times10^{34}$ m$^{-3}$, $n_{e0} = 1.23\times10^{37}$ m$^{-3}$, $T = 6.5\times10^9$ K, $m_i = 56$ a.m.u, and $Z_i = 1, 2, 3$ for Fe (I), Fe (II), and Fe (III) ions, respectively. Other parameters are $\Delta m^2c^4 = 3\times10^{-5}$ eV$^2$, $\sin(2\theta_0) = 10^{-1}$, and $G_{\rm F} = 1.45\times10^{-62}$ J m$^3$. For these parameters, the electron Fermi energy is much larger than both the thermal energy ($E_{\rm Fe} \gg k_BT_e$) and the rest mass energy of the electrons ($E_{\rm Fe} \gg m_ec^2$). Hence, the assumption of ultrarelativistic and degenerate electrons is justified, which is also the case for a dense iron core of a massive star at the last stage of stellar evolution. It has also been proposed in an earlier study that the neutrino-beam-driven instability growth rate is larger for perpendicular propagation of the neutrino beam with respect to the plasma waves (Prajapati 2017). However, for the considered set of parameters in the present study, it is found that the condition (25) is satisfied for a particular value of angle ($\theta$) between the direction of the IAWs and the neutrino beam, which is $\theta \approx 89.72°$ for ultrarelativistic degenerate electrons and Fe(II) ions. Hence, it is clear that the neutrino-driven instability growth rate attains a maximum value for a near-perpendicular propagation of the neutrino beam with respect to the IAWs. For the considered set of parameters, we obtain the eigenfrequency of the neutrino flavor oscillations as $\Omega_\nu = 6.3\times10^9$ rads$^{-1}$ and the ion acoustic speed as $V_s = 1.49\times10^6$ m s$^{-1} \ll c$. The critical wavenumber for the neutrino-driven instability is evaluated to be $k = 4.2\times10^3$m$^{-1}$; hence, the neutrino-driven instability will be significant for large-wavenumber or short-wavelength perturbations. The time period of the instability growth for the considered parameters is numerically determined using MATHEMATICA from the positive imaginary root of Equation (26) and is found to be

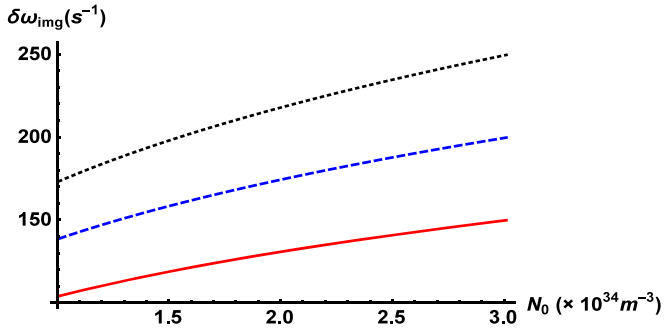


**Figure 1.** Variation of the growth rate of the neutrino-driven instability with the number density $N_0$ of the neutrino beam for different values of the eigenfrequency $\Omega_\nu$ of the neutrino flavor oscillations. Red (solid) curve: $\Omega_\nu = 3 \times 10^9$ rad s$^{-1}$; blue (dashed) curve: $\Omega_\nu = 4 \times 10^9$ rad s$^{-1}$; black (dotted) curve: $\Omega_\nu = 5 \times 10^9$ rad s$^{-1}$. The other parameters are $\mathcal{E}_0 = 1.94$ MeV, $\theta = 89.^\circ72$, $n_{e0} = 3.23 \times 10^{37}$ m$^{-3}$, $Z_i = 2$, $m_i = 56$ a.m.u.

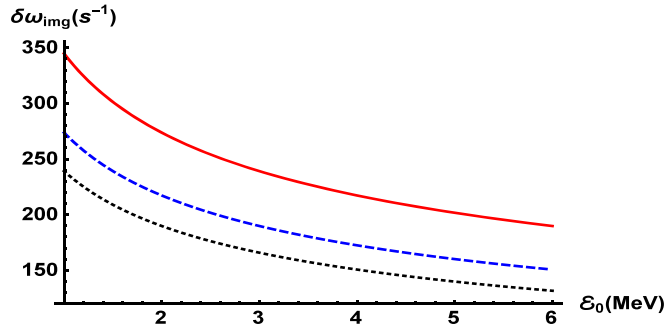


**Figure 2.** Variation of the growth rate of the neutrino-driven instability with energy $\mathcal{E}_0$ of the neutrino beam for different charge states $Z_i$ of iron. Red (solid) curve: $Z_i = 1$; blue (dashed) curve: $Z_i = 2$; black (dotted) curve: $Z_i = 3$. The other parameters are $N_0 = 1.03 \times 10^{34}$ m$^{-3}$, $n_{e0} = 3.23 \times 10^{37}$ m$^{-3}$, $\theta = 89.^\circ72$, $m_i = 56$ a.m.u.

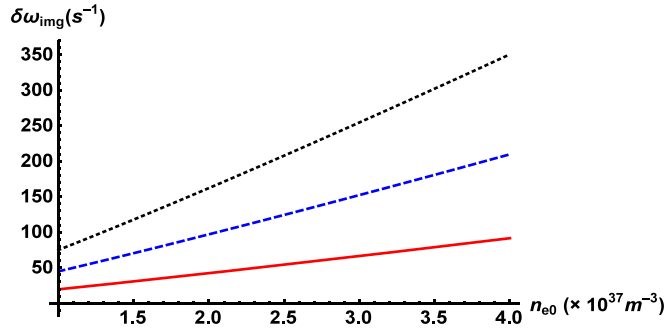


**Figure 3.** Variation of the growth rate of the neutrino-driven instability with the electron number density $n_{e0}$ for different values of the ion mass $m_i$. Red (solid) curve: $m_i = 1$ a.m.u.; blue (dashed) curve: $m_i = 12$ a.m.u.; black (dotted) curve: $m_i = 56$ a.m.u. The other parameters are $N_0 = 1.03 \times 10^{34}$ m$^{-3}$, $\mathcal{E}_0 = 1.94$ MeV, $Z_i = 1$, $\theta = 89.^\circ72$.

≈4.5 ms, which is small enough to alter the dynamics of supernova explosion due to core collapse of a progenitor star.

The dependence of the growth rate $\delta\omega_{\rm img}$ of the neutrino beam instability on the different physical parameters is depicted in Figures 1–3. The influence of neutrino flavor oscillations and the number density of the neutrino beam on the instability growth rate is presented in Figure 1. It is shown that with an increase in the eigenfrequency of the neutrino flavor oscillations and the number density of the neutrinos, the instability growth becomes more rapid. It is inferred that as the eigenfrequency of the neutrino flavor oscillations resonates with the frequency of IAWs, the instability growth rate is significantly enhanced, which may be due to an increased energy exchange between the neutrino beam and the ion acoustic waves. It is clear that the neutrino flavor oscillations have a significant influence on the neutrino-driven instability phenomenon.

The variation of the neutrino-driven instability growth rate with the neutrino energy for different values of the ion charge number is depicted in Figure 2. It is seen that the growth rate of the instability decreases with an increase in energy of the neutrino beam. In other words, the enhanced energy of the neutrino beam has a stabilizing influence on the neutrino-driven streaming instability. It is also noticeable from Figure 2 that for a higher ion charge state, the neutrino-driven instability growth rate decreases. Hence, the IAWs become more rapidly unstable if the abundant ion species are iron with the charge state Fe (I) compared to Fe (II) and Fe (III).

The influence of the number density of ultrarelativistic, degenerate electrons on the instability of IAWs in the presence of neutrinos is illustrated in Figure 3. It is seen that an enhancement in the number density of ultrarelativistic degenerate electrons tends to an increase of the growth rate of the neutrino-driven instability ($\delta\omega_{\rm img}$). In other words, the dense, degenerate core of a progenitor star gets destabilized in a much shorter time if the electron gas interacting with the streaming neutrino beam is denser. The effect of different ion species on the neutrino beam instability is also seen in Figure 3. It is remarked that the ion species play a prominent role for the instability criterion of the IAWs in the present case. As the ion species become more massive, for example, as the concentration of the dense core plasma and its surrounding layers is changed when carbon gets converted into iron, the neutrino instability growth is significantly increased. It is concluded that the neutrino beam instability is most prominent if a dense neutrino beam having minimal energy interacts with an electron dense progenitor core containing iron as a major trace element.

## 5. Conclusions

We have investigated the neutrino-driven instability mechanism by considering neutrino flavor oscillations in a plasma containing cold, heavy ions and electrons that are relativistic and degenerate. The instability phenomenon is studied with its relevance to the core-collapse supernova explosion by considering physical parameters of the advanced stages of a progenitor star. It is observed that the neutrino parameters such as the energy and number density of neutrinos and the eigenfrequency of neutrino flavor oscillations have a profound influence on the neutrino-driven instability growth rate. The time period of the neutrino-driven instability process is of the order of a few milliseconds and hence the instability is fast enough to alter the dynamics of a core-collapse supernova explosion that occurs at the timescale of few seconds. The findings of this study of plasma wave instability due to a neutrino beam carrying out flavor oscillations gives new insights into understanding the process of core-collapse supernova and in predicting the dominant mechanism for the collapse.

This work was supported by DRS-II (SAP) No. F/530/17/DRS-II/2015(SAP-I) University Grants Commission (UGC), New Delhi, India. Y.G. gratefully acknowledges University

Grants Commission (UGC) for providing scholarship under Basic Scientific Research (BSR) scheme.

## ORCID iDs

Yashika Ghai https://orcid.org/0000-0002-8432-0233
N. S. Saini https://orcid.org/0000-0001-7739-8377
B. Eliasson https://orcid.org/0000-0001-6039-1574

## References

Bethe, H. A. 1986, PhRvL, 56, 1305
Bingham, R., Bethe, H. A., Dawson, J. M., Shukla, P. K., & Su, J. J. 1996, PhLA, 220, 107
Bingham, R., Dawson, J. M., Su, J. J., & Bethe, H. A. 1994, PhLA, 193, 279
Chandrasekhar, S. 1935, MNRAS, 95, 207
Chiueh, T. 1993, ApJL, 413, L35
Connor, E. O. 2015, ApJS, 219, 24
Eliasson, B., & Shukla, P. K. 2012, EL, 97, 15001
Fröhlich, C., Perego, A., Hempel, M., et al. 2018, J. Phys.: Conf. Ser., 940, 012001
Haas, F. 2016, JPlPh, 82, 705820602
Haas, F., & Eliasson, B. 2015, PhyS, 90, 088005
Haas, F., Pascoal, K. A., & Mendonça, J. T. 2017a, PhRvE, 95, 013207
Haas, F., Pascoal, K. A., & Mendonça, J. T. 2017b, PhPl, 24, 052115
Hirata, K., Kajita, T., Koshiba, M., et al. 1987, PhRvL, 58, 1490
Iqbal, M. J., Shah, H. A., Masood, W., & Tsintsadze, N. L. 2018, EPJD, 72, 192
Jankaa, H.-Th., Langanke, K., Marek, A., et al. 2007, PhR, 442, 38
Khan, S. A., Din, B. U., Ilyas, M., & Wazir, Z. 2016, Prama, 86, 1143
Masud, M. M., & Mamun, A. A. 2013, Prama, 81, 169
Mendonça, J. T., & Haas, F. 2013, PhPl, 20, 072107
Mendonça, J. T., Haas, F., & Bret, A. 2014, PhPl, 21, 092117
Mezzacappa, A., & Messer, O. E. B. 1999, JCoAM, 109, 281
Mikheev, S. P., & Smirnov, A. Y. 1986, JETP, 64, 4
Mikheev, S. P., & Smirnov, A. Y. 1987, SvPhU, 30, 759
Ott, C. D., Roberts, L. F., Schneider, A. S., et al. 2018, ApJL, 855, L3
Prajapati, R. P. 2017, PhPl, 24, 122902
Rahman, A., Qamar, A., Naseer, S., & Naeem, S. N. 2017, CaJPh, 95, 655
Serbeto, A. 1999, PhPl, 6, 2943
Serbeto, A., Shukla, P. K., & Monteiro, L. F. 2002, PPCF, 44, L43
Sharma, P. 2018, PhLA, 382, 1796
Shukla, P. K., Silva, L. O., Bethe, H., et al. 1999, PPCF, 41, A699
Silva, L. O., Bingham, R., Dawson, J. M., Mendonça, J. T., & Shukla, P. K. 1999, PhRvL, 83, 2703
Silva, L. O., Bingham, R., Dawson, J. M., Mendonça, J. T., & Shukla, P. K. 2000, ApJS, 127, 481
Smirnov, A. Yu. 2005, PhyS, T121, 57
Yoshida, T., Takahashi, K., & Umeda, H. 2016, J. Physics: Conference Series, 718, 062073